A Numerical Study on Dynamic Characteristics of a Catenary

Woonkyung M. Kim
Department of Radio Communications Engineering, College of Information and Communications, Korea University, Seoul 136-701, Korea
Jeung Tae Kim, Jung Soo Kim*
Department of Mechanical and System Design Engineering, College of Engineering, Hongik University, 72-1 Sangsu-dong Mapo-gu, Seoul 121-797, Korea
Jae Won Lee
Graduate School, College of Engineering, Hongik University, 72-1 Sangsu-dong Mapo-gu, Seoul 121-797, Korea

Dynamic characteristics of a catenary that supplies electrical power to high-speed railway is investigated. The catenary is a slender structure composed of repeating spans. Each span is in turn composed of the contact and messenger wires connected by the hangers in regular intervals. A finite element based dynamic model is developed, and numerical simulations are performed to determine the dynamic characteristics of the catenary. The influence of the structural parameters on the response characteristics is investigated. The structural parameters considered include tension on the contact and messenger wires, stiffness of the hangers, and the hanger and span spacing. The hanger characteristics are found to be the dominant factors that influence the overall dynamic characteristics of the catenary.

Key Words : Catenary, Contact Wire, Finite Element Model, Wave Propagation, Frequency Response Function, High-speed Railway

1. Introduction

Interest in high speed trains has risen in recent years due to their convenience, speed, and safety. The electrical power required for train traction is supplied by the catenary. The catenary is a slender structure composed of up to ten repeating spans. Each span is composed of the contact and messenger wires connected by thin wires known as the hangers in regular intervals. The catenary is supported by posts known as the catenary support at the boundary between the adjoining spans. To keep in pace with ever increasing train speed, the catenary design seeks to maintain uniform compliance under high tension.

In developing necessary technologies, numerical simulation of the catenary dynamics has become an important tool for supplementing experimental investigations which are quite cumbersome to conduct due to high cost and difficulty in securing track time for test runs. The numerical simulation can often serve as a useful and economical tool for performing sensitivity analysis of the structural parameters and helping to obtain optimal design solutions.

A number of research works related to the performance of the catenary have been reported in open literature. In the early works of Farr et al. (1961) and Willets et al. (1966), dynamic analyses of the catenary for low-speed rail applications were carried out based on experimental data collected from scaled-down models. Later,

* Corresponding Author,
E-mail : jungsoo@wow.hongik.ac.kr
TEL : +82-2-320-1471; **FAX** : +82-2-322-7003
Department of Mechanical and System Design Engineering, College of Engineering, Hongik University, 72-1 Sangsu-dong Mapo-gu, Seoul 121-797, Korea.
(Manuscript **Received** December 26, 2002; **Revised** March 11, 2003)

Manabe (1989) reported on experimental investigations for high-speed applications based on a scaled-down model of the catenary. Manabe (1991) also investigated design changes needed in the catenary to accomodate increase in train speed. Delfosse and Sauvestre (1983) focused on improving the reliability of the experimental methods for measuring the vertical motion of the contact wire. In the early analytical work of Belyaev and Vologine (1977), a simple discrete model of the catenary was developed to examine the influence of the dynamic parameters on the catenary response. Later, Chung and Choi (1991) performed numerical analysis of the catenary dynamics in which the contact and messenger wires were modeled as uniform strings under tension. Kim et al. (1992) investigated wave propagation characteristics of the catenary by applying the finite difference method on a dynamic model in which the contact and messenger wires were modeled as uniform strings under tension. On the train side, Seering et al. (1991) investigated the design issues that need to be addressed to ensure steady supply of electrical current from the catenary. More recently, Park et al. (1999) looked into the vibration responses of the catenary by considering various disturbances that can occur due to train motion.

In the present study, numerical analysis of the catenary based on a finite element model is presented. The contact and messenger wires are modeled as tensioned-beam elements to better account for flexural rigidity of these wires. The organization of the paper is as follows. In section 2, a dynamic model of the catenary based on the finite element formulation is described. In section 3, results of the numerical simulation are presented, followed by an examination of the effect of the structural parameters on the catenary response, reported in section 4. Finally, the main results are summarized in section 5. The nominal input values used for the simulation runs are based on the specifications of the Korean High Speed Rail System.

2. Mathematical Modeling

The overall structure of the catenary is shown in Fig. 1. The electrical current is supplied to the train through the contact wire. The contact wire is connected to the messenger wire through the hangers that serve to transmit weight of the contact wire onto the messenger wire. The hanger is a thin cable with uniform density and large stiffness in tension and negligible stiffness in compression. The messenger wire is supported by the catenary support, and the hanger lengths are set such that the contact wire profile maintains flatness within a proscribed limit. To properly account for the high frequency modes, the contact and messenger wires are modeled as beams under tension possessing flexural rigidity instead of the string elements adopted in the previous investigations.

The hangers are modeled as uniform cable elements that transmit the weight of the contact wire onto the messenger wire by connecting the two wires. Depending on the range of the relative motion of the contact and messenger wires, the hangers need to be modeled differently. In the static equilibrium position, the hangers are under elastic deformation (elongated) due to the weight of the contact wire. For small relative motion, the hanger always stay elongated due to the pull of the contact wire. Therefore, for small catenary motion, the hangers are always in tension and should be modeled as linear springs. There are intermittent occasions, however, in which the

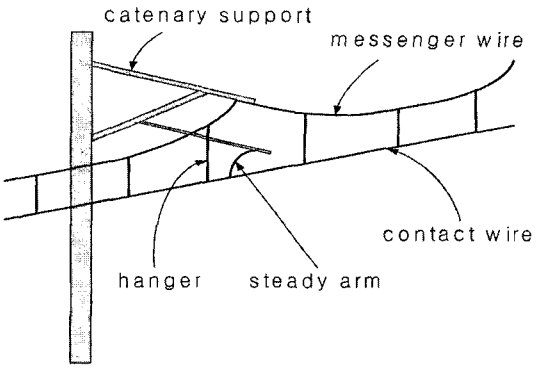

Fig. 1 Structure of catenary

relative motion between the contact and messenger wires is such that the hanger goes into compression. If the relative motion of the wires is such that the distance between the two wires gets shorter than the unstretched length of the hanger, the hangers will go into compression. For such cases, the hanger stiffness during compression becomes almost negligible, and the hangers need to be modeled as nonlinear springs with a bi-directional stiffness property. Such cases will be referred to as large catenary motion.

The steady arm is used to provide lateral adjustment on the contact wire, and can be treated simply as a lumped mass for the vertical motion analysis purpose. The catenary support can be treated as a cantilever beam, and the equivalent spring-mass can be computed and incorporated into the model. One-half of each hanger mass is appended to the contact wire and the other half to the messenger wire as lumped masses. There are nine hangers for each span. The resulting finite element model of the catenary structure is shown in Fig. 2. The figure shows the 3-span model with the span length of 63 m. Clamped boundary conditions are applied at both ends of the structure. The 6-span model was also constructed and identical simulations were run on both the 3-span and 6-span models, with no difference noted in the main conclusions reached. The later analyses will demonstrate that the number of the spans in the catenary model in excess of three has no bearing on the overall dynamic characteristics of the catenary.

From the finite element model, the global equations of motion of the catenary can be cast in the form of

$$[M]\{\ddot{u}(t)\}+[C]\{\dot{u}(t)\}+[K]\{u(t)\}=F(t) \quad (1)$$

where M, C, K matrices are the system mass, damping, and stiffness matrices, and $u(t)$ and $F(t)$ denote the displacement response vector and excitation vector, respectively. The matrices are all banded and symmetric, and Wilson-θ integration scheme is applied to obtain the solutions. (for general discussion, see Bathe, 1982) The specifications of the Korean High Speed Rail System catenary used during modeling are listed in Table 1, and the damping ratios for the contact and messenger wires are set at 5% and 1%, respectively.

Table 1 Specifications of the Korean High Speed Rail System catenary

	Contact wire	Messenger wire
T	20000 N	14000 N
E	1.18×10^{11} Pa	1.10×10^{11} Pa
ρ	8.893×10^{3} kg/m^3	9.238×10^{3} kg/m^3
A	0.000150 m^2	0.00006549 m^2

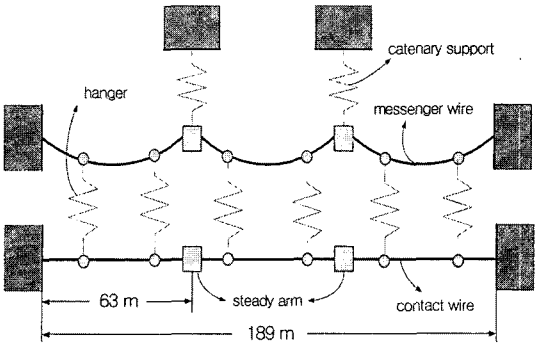

Fig. 2 3-span catenary model

3. Dynamic Analysis of Catenary

Responses of the finite element model of the catenary for the linear hanger stiffness case, i.e., for small catenary motion, is simulated. The hanger spring constant is set at 10^5 N/m. The impulse responses of the contact wire in the frequency domain are shown in Figs. 3 and 4. An impulse is applied at the center of the catenary and the responses are calculated at the same point. The figures show that for the displacement response, 1.0 Hz component is dominant while for the acceleration response, 10.5 Hz and 21.0 Hz components are pronounced. In the following analysis, these components are found to be closely related with the spacing (horizontal distance) between the adjacent spans and hangers, respectively. They arise from the reflections of the propagating wave at the span and hanger boundaries.

If the contact and messenger wires are treated as separate tensioned-beam structures, the wave

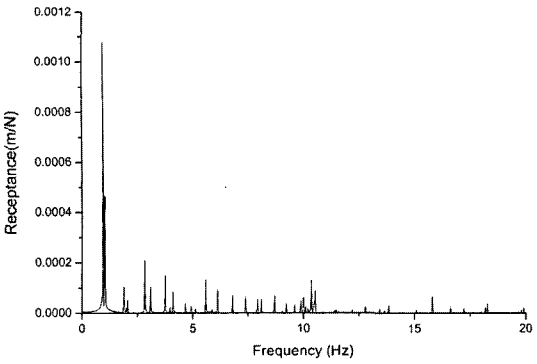

Fig. 3 Displacement FRF-linear hanger stiffness model

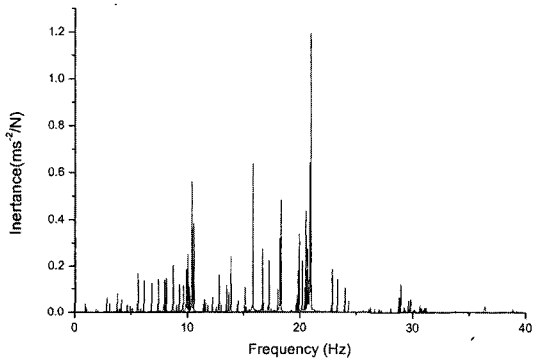

Fig. 4 Acceleration FRF-linear hanger stiffness model

propagation velocity can be calculated by (Petyt, 1990)

$$c=\sqrt{\frac{T}{2\rho A}+\left[\left(\frac{T}{2\rho A}\right)^2+\left(\frac{EI}{\rho A}w^2\right)\right]^{1/2}} \quad (2)$$

where c, T, ρ, A, and w denote the wave propagation velocity, tension in the wire, mass density, cross-sectional area, and the circular frequency of the propagating wave, respectively. For tensioned-beams, the propagation velocity is dependent on the frequency of the wave due to its beam-like nature. In the present case, this dependence is somewhat slight, and for the frequency range of 0 to 50 Hz, the contact wire has the calculated velocity in the range of 122.4 m/s~122.9 m/s while the messenger wire has the velocity range of 152.1 m/s~153.0 m/s, yielding the mean propagation velocities of 122.7 m/s and 152.6 m/s, respectively. For the catenary structure in which the contact and messenger wire dynamics are coupled, however, simulated wave propagation velocities are significantly different: The mean contact wire wave propagation velocity increases to 135 m/s while the mean velocity for the messenger wire decreases to 136 m/s, implying that the wave propagation velocities have converged due to coupling effect of the hangers. For a given wave propagation velocity, the frequency corresponding to the wave traversing a segment of length l back and forth can be calculated by

$$f=\frac{\gamma c}{2\pi}=\frac{\frac{2\pi}{\lambda}c}{2\pi}=\frac{c}{\lambda}=\frac{c}{2l} \quad (3)$$

where f, l, λ, and γ denote the frequency, length, wave length, and wave number, respectively. Substituting the wave propagation velocity of 135 m/s and the span length of 63 m into Eq. (3) yields 1.0 Hz. Substituting the spacing between the adjacent hangers of 6.65 m yields 10.5 Hz, and by multiplying by 2, 21.0 Hz can be obtained as well. The dominant 1.0 Hz component of the contact wire displacement response shown in Fig. 3 is related to the wave reflections from the span boundary, while the dominant frequency components of the acceleration response shown in Fig. 4 are due to the wave traversing between the adjacent hangers.

To further verify the above observations, the harmonic excitations with frequencies of 1.0 Hz, 10.5 Hz, and 21.0 Hz, respectively, are applied at the center of the catenary model and the responses are calculated as functions of the distance along the contact wire. In Fig. 5, the effect of the span boundaries on the response of the contact wire for the 1.0 Hz harmonic excitation is clearly visible. The two vertical lines in the figure denote the span boundaries. In Figs. 6 and 7, the responses of the middle span segment for the 10.5 Hz and 21.0 Hz harmonic excitations are shown. The nine vertical lines represent the hanger boundaries within the middle span. In both figures, the response contours clearly show the dependence on the hanger boundaries. It is known from the investigation of Park et al. (1999) that 10.5 Hz and 21.0 Hz frequency components play an important role on the issue of maintaining contact

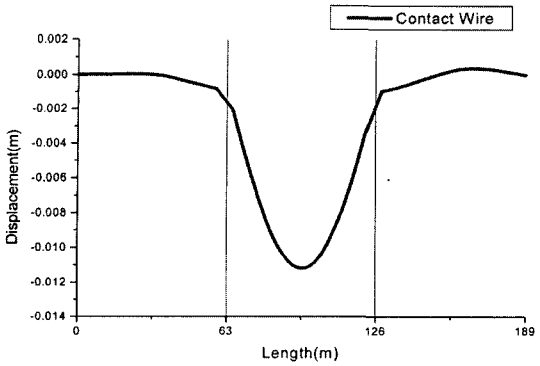

Fig. 5 1.0 Hz harmonic response

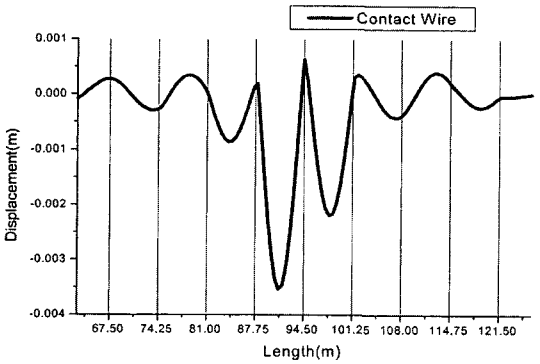

Fig. 6 10.5 Hz harmonic response

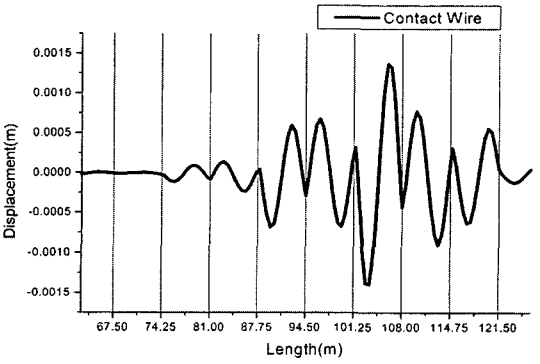

Fig. 7 21.0 Hz harmonic response

between the catenary and the running train. The simulation runs were also conducted using the 6-span model with no difference in the main findings.

In order to better understand the above findings, the modal properties are investigated. For slender, repeating structures such as the catenary, a large number of modes exist with small spacing

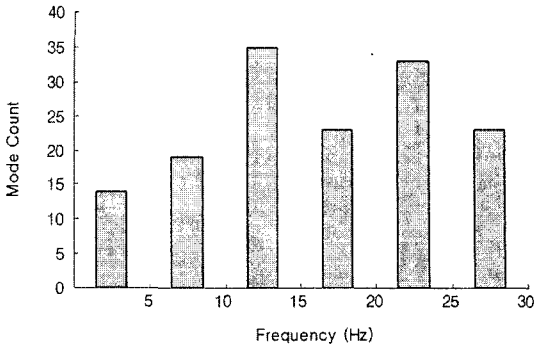

Fig. 8 Modal density

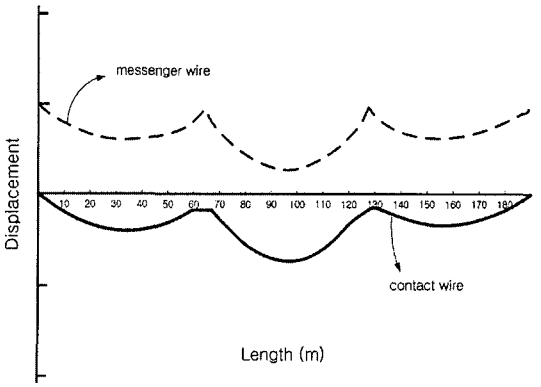

Fig. 9 First mode shape

between the adjacent modes in the frequency domain. It is more appropriate in this case to consider the modal density instead of individual modes, as shown in Fig. 8 for the 3-span model. For simple tensioned-beam structures, fairly uniform (albeit slightly decreasing) modal distribution can be expected. For the catenary structure however, the modal distribution is quite uneven, with higher modal density observed in certain frequencies. These frequencies seem to be related with the acceleration response of Fig. 4. This relationship can be explained by the concept of the statistical energy analysis (SEA) in which the vibration energy level in a given frequency range is assumed to be proportional to the number of modes present in the range. (for general discussion, see Lyon, 1975) Although the frequency range considered in the present study is lower than the range in which the statistical energy analysis is usually applied, a sufficient number of modes exist in this case for the correlation be-

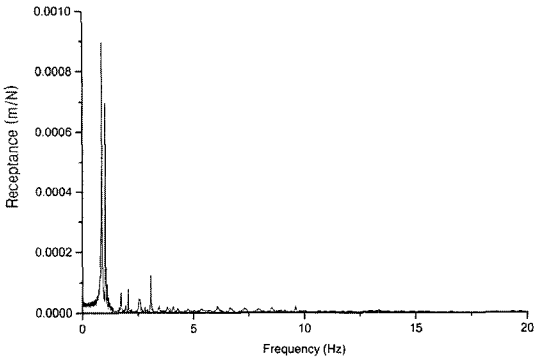

Fig. 10 Displacement FRF-nonlinear hanger stiffness model

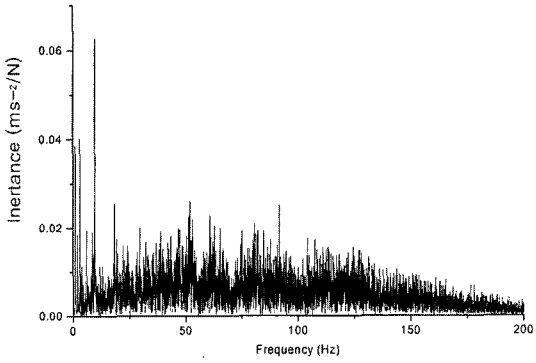

Fig. 11 Acceleration FRF-nonlinear hanger stiffness model

tween the vibration energy level and the modal density to be significant. For 6-span model, the modal density is approximately double that of Fig. 8 but the modal distribution is quite similar, and the identical conclusion is reached. A representative mode shape is illustrated in Fig. 9.

In the static equilibrium position of the catenary, each hanger is subject to 92 N tensile force due to the gravitational pull of the catenary wire, resulting in the approximately 1 mm elastic deformation of the hanger. When the relative displacement between the contact and messenger wires exceeds the 1 mm static deformation initially in place, perhaps due to a jerking motion of the contact wire, the hangers need to be modeled as bi-directional springs with the spring constants of 105 N/m during tension (just as in the linear stiffness model) and 10 N/m during compression (negligible stiffness). The simulated results of the

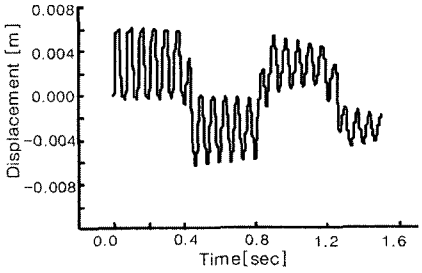

Fig. 12 Transient response-linear hanger stiffness model

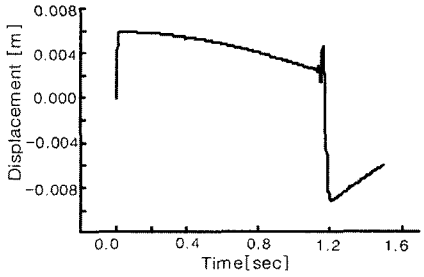

Fig. 13 Transient response-nonlinear hanger stiffness model

catenary model with the nonlinear hanger stiffness are shown in Figs. 10 and 11. As in the linear case shown in Figs. 3 and 4, the dominant frequency components at 1.0 Hz and 10.5 Hz are visible. There is an important difference, however, in that the response energy is more widely spread in the frequency domain. This implies that there is less vibration energy at the low frequency range which normally plays more dominant role in the catenary motion. This finding is corroborated by comparing the transient responses of the linear and nonlinear catenary models as shown in Figs. 12 and 13. The dominant period of the transient response shown in Fig. 12 corresponds to the 10. 5Hz component of Fig. 4. In contrast, the response shown in Fig. 13 for the nonlinear case lacks distinct periodicity.

4. Effect of Structural Parameters on Catenary Dynamics

To more closely examine the sensitivity of the catenary response on the structural parameters, the nominal design values of these parameters are varied, and the corresponding variations in the

responses are calculated.

4.1 Effect of tension

For the frequency range of less than 50 Hz, the magnitude of $\frac{EI}{\rho A} w^2$ term in Eq. (2) is less than 2.7% of $\frac{T}{2\rho A}$ term, implying the predominance of the tension effect over the flexural rigidity effect in the contact and messenger wires considered here. Therefore, the rate of the wave propagation velocity variation should more or less be proportional to $\sqrt{T}$ in close agreement with uniform strings. Varying the tension in the wire affects the wave propagation velocity and causes the corresponding variation in the dynamic characteristics such as the natural frequency. The wave propagation velocity of the contact wire as a function of the tension is plotted in Fig. 14. The wave propagation velocity of a uniform string which exactly follows the $\sqrt{T}$ rule is also plotted for comparison, and the two curves are quite similar. The variation in the 21 Hz frequency component

Table 2 Wave propagation velocity and frequency vs. tension

Tension in contact/messenger wires (% change from nominal value)	Simulated propagation velocity (m/s)	Propagation velocity of simple wire (m/s)	Frequency due to hanger spacing (Hz)
10000/7000(−50)	95.0	86.58	14.2
14000/9800(−30)	112.5	102.44	17.3
18000/12600(−10)	127.3	116.16	19.0
20000/14000(0)	135.0	122.44	21.0
26000/18200(+30)	154.0	139.4	23.6

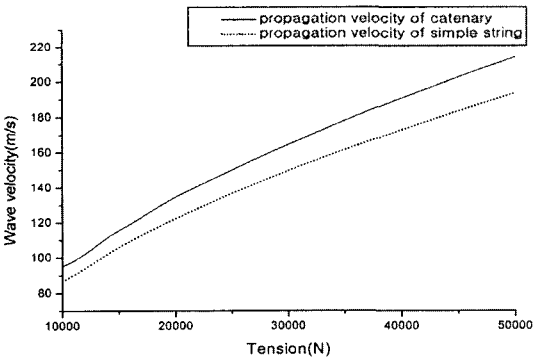

Fig. 14 Wave propagation velocity vs. tension

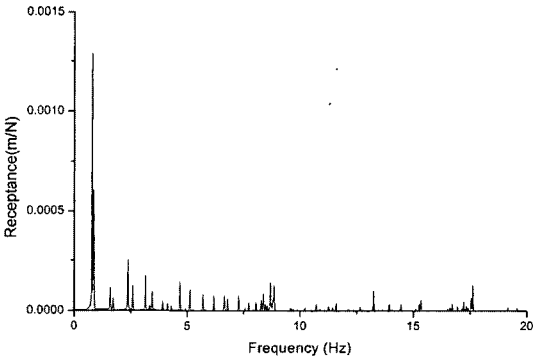

Fig. 15 Displacement FRF-tension reduced by 30%

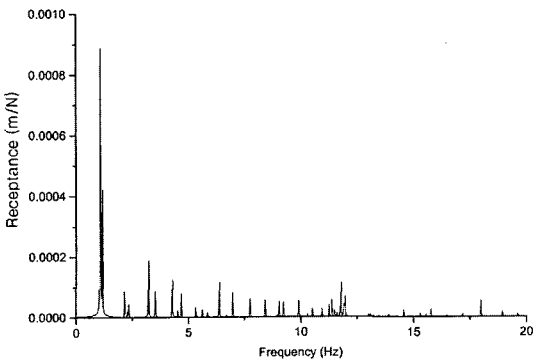

Fig. 16 Displacement FRF-tension increased by 30%

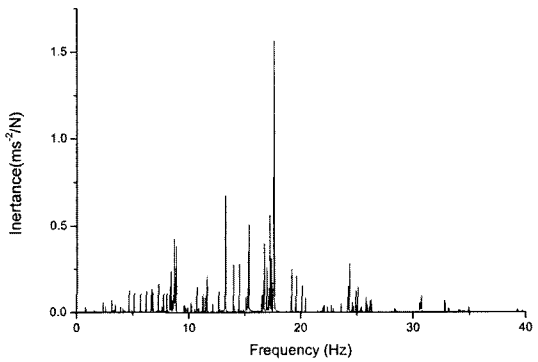

Fig. 17 Acceleration FRF-tension reduced by 30%

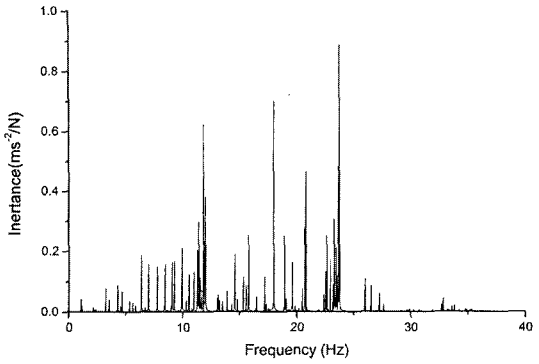

Fig. 18 Acceleration FRF-tension increased by 30%

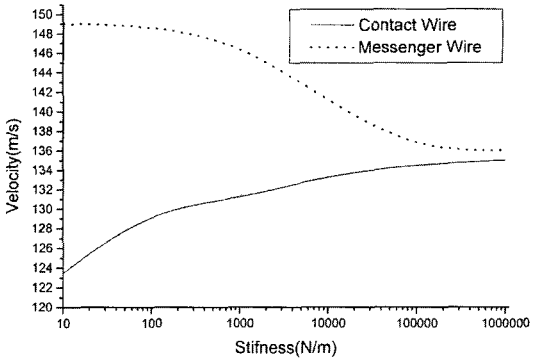

Fig. 19 Wave propagation velocity vs. hanger stiffness-linear model

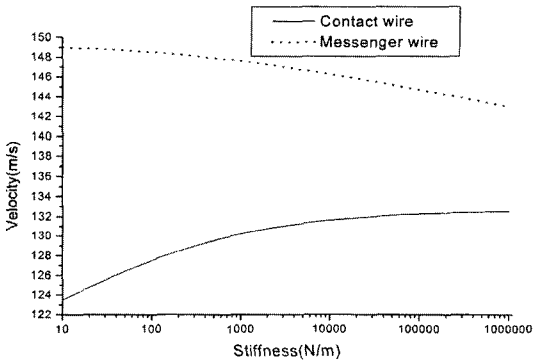

Fig. 20 Wave propagation velocity vs. hanger stiffness-nonlinear model

related with the hanger spacing of the catenary is listed in Table 2. It varies in direct proportion to the wave propagation velocity. According to Figs. 15 through 18, all major frequency components of the response vary in direct proportion to the wave propagation velocity.

4.2 Effect of hanger stiffness

It was noted in Section 3 that the wave propagation velocities for the contact and messenger wires in the catenary are significantly different from those of the wires calculated by treating them as separate structures: They converge due to the coupling effect of the hangers. Figs. 19 and 20 further explore this issue by plotting the wave propagation velocities as functions of the hanger stiffness. For the linear model shown in Fig. 19, the two propagation velocities are initially distinct for low hanger stiffness but converge as the hanger stiffness is increased. Once the wave propagation velocity has converged, the frequency components corresponding to the reflections of the disturbance wave at the span and hanger boundaries become predominant. For the nonlinear model of Fig. 20 in which the hanger stiffness in compression is fixed at 10 N/m and only the stiffness in tension is varied, the coupling effect of the hanger is diminished and no convergence is observed. The net result is that the influence of the span and hanger boundaries on the dynamic responses of the catenary is diminished as well. This result also explains in part wider frequency spectrums of the responses observed in Figs. 10 and 11 for the nonlinear case. Since the contact and messenger wires maintain distinct wave propagation velocities, the number of frequency components associated with Eq. (3) is greater.

To examine this issue in greater depth, the linear hanger stiffness is artificially set at 10 N/m to induce minimal coupling between the contact and messenger wires. Figure 21 shows a more widely spread response spectrum, thus vindicating the supposition. It is also noted that the 10.5 Hz and 21.0 Hz frequency components of Fig. 4 decrease to 9.4 Hz and 18.8 Hz, respectively, in direct proportion to the downward shift in the wave propagation velocity of the contact wire. The displacement of the contact wire is shown in Fig. 22. While the spread in the response spectrum is not as obvious as in the acceleration response, the predominance of the 1.0 Hz component related with the span boundary vanishes. In addition,

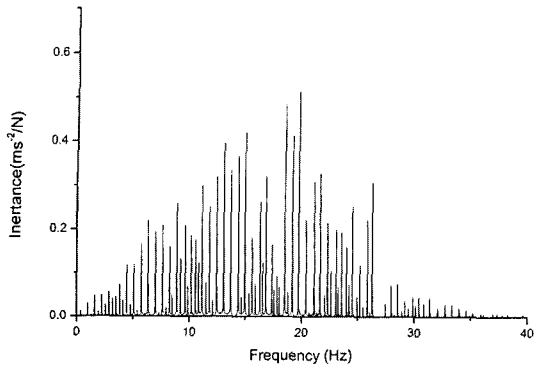

Fig. 21 Acceleration FRF-hanger stiffness of 10 N/m

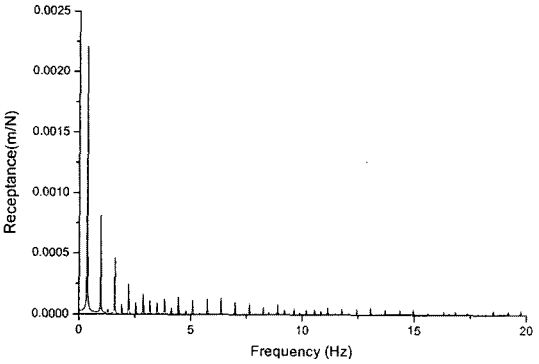

Fig. 22 Displacement FRF-hanger stiffness of 10 N/m

there is a pronounced increase in the magnitude of the displacement. Normally, a strong coupling allows the messenger wire to shoulder a significant portion of the excitation load, thus easing the burden on the contact wire. When the coupling is diminished due to low stiffness, the sharing of the burden cannot take place as readily, and results in greater motion of the contact wire.

4.3 Effect of hanger spacing

It was previously noted that the hangers act to transfer a portion of the dynamic load acting on the contact wire onto the messenger wire. The degree of such transfer increases in direct proportion to the number of the hangers available. The number of the hangers for each span is varied and the corresponding displacement of the contact wire listed in Table 3. As the number of the hangers increases, i.e., the spacing between the hangers decreases, the contact wire compliance achieves more homogeneity, and the displacement magnitude decreases. The frequency of the wave reflecting from the hanger boundary is inversely proportional to the spacing, and is also listed in Table 3.

Table 3 Response characteristics for different hanger numbers

No. of hangers/span	Hanger spacing (m)	Contact wire displacement (mm) at 90 m	Frequency (Hz)
6	9	10.311	7.4/14.9
9	6.75	9.961	10.5/21.0
12	5.0	9.919	13.2/26.4

5. Conclusions

Dynamic characteristics of the catenary that supplies electrical power to high-speed railway is numerically investigated. A finite element based model of the catenary that incorporates the flexural rigidity of the contact and messenger wires is developed, and numerical simulations are conducted by varying the structural parameters. The hanger is found to play predominant role in determining the structural characteristics of the catenary by inducing coupling between the contact and messenger wires.

For small catenary motion, i.e., for the linear hanger stiffness case, the reflections of the propagating disturbance wave at the span and hanger boundaries are found to determine the major frequency components of the dynamic response of the catenary. For large catenary motion, i.e., for the nonlinear hanger stiffness case, the response is spread across much wider spectrum, with significant amount of high frequency components present in the dynamic response of the catenary.

Acknowledgment

The authors are grateful for the support provided by a grant from Korea Science and Engi-

neering Foundation (KOSEF).

References

Bathe, K. J., 1982, *Finite Element Procedures in Engineering Analysis*, Prentice-Hall.

Belyaev, I. A., Vologine, V. A. and Freidfeld, A. V., 1977, "Improvement of Pantographs and Catenaries and Method of Calculating their Mutual Interactions at High Speed," *Rail International*, pp. 309~328.

Chung, D. H., Choi, Y. S., 1991, "Numerical Analysis of Dynamic Response of Catenary/Pantograph System in High Speed Train," *J. Sungkyunkwan Univ.*, Vol. 24, No. 1, pp. 377~390.

Delfosse, P., Sauvestre, B., 1983, "Measurement of Contact Pressure between Pantograph and Catenary," *French Railway Review*, Vol. 1, No. 6, pp. 497~505.

Farr, D. S., Hall, H. C., Williams, A. L., 1961, "A Dynamic Model for Studying the Behaviour of the Overhead Equipment used in Electric Railway Traction," *Proc. IEE*, No. 3530U, pp. 421~434.

Kim, Y. H., Park, Y. K., Kim, S. M. and Roh, H. S., 1992, "Wave Propagation Characteristics along a Catenary with Arbitrary Boundary Conditions," *Trans. KSME*, Vol. 16, No. 11, pp. 2059~2071.

Lyon, R. H., 1975, *Statistical Energy Analysis of Dynamic Systems : Theory and Application*, MIT Press.

Manabe, K., 1989, "High-Speed Contact Performance of a Catenary-Pantograph System (An Experiment Study Using a Dynamically Scaled Model)," *JSME International Journal*, Vol. 32, No. 2, pp. 200~205.

Manabe, K., 1991, "Catenary-Pantograph System Dynamics for Speedup of Shinkansen," *RTRI Quarterly*, Vol. 33, No. 1, pp. 39~45.

Park, S. H., Kim, J. S., Hur, S., Kyung, J. H. and Song, D. H., 1999, "Vibration Response of TGV-K Catenary System Subject to External Forces," *Proc. KSNVE*, pp. 448~454.

Petyt, M., 1990, *Introduction to Finite Element Vibration Analysis*, Cambridge University Press.

Seering, W., Armbruster. K., Vesely, C. and Wormley, D., 1991, "Experimental and Analytical Study of Pantograph Dynamics," *J. Dynamic Systems, Measurement, and Control*, Vol. 113, pp. 242~247.

Willets, T. A. and Edwards, D. R., 1966, "Dynamic-model Studies of Overhead Equipment for Electric Railway Traction," *Proc. IEE*, Vol. 113, No. 4, pp. 690~696.